Biochemical Pharmacology 85 (2013) 1182–1194

Contents lists available at SciVerse ScienceDirect

Biochemical Pharmacology

journal homepage: www.elsevier.com/locate/biochempharm

Characterization of marmoset CYP2B6: cDNA cloning, protein expression and enzymatic functions

Kei Mayumi [a], Nobumitsu Hanioka [a], Kazufumi Masuda [b], Akiko Koeda [c], Shinsaku Naito [d], Atsuro Miyata [e], Shizuo Narimatsu [a,*]

[a] Laboratory of Health Chemistry, Graduate School of Medicine, Dentistry and Pharmaceutical Sciences, Okayama University, Okayama, Japan
[b] Graduate School of Clinical Pharmacy, Shujitsu University, Okayama, Japan
[c] Ina Research Inc., Nagano, Japan
[d] Otsuka Pharmacutical Factory, Inc., Tokushima, Japan
[e] Department of Pharmacology, Graduate School of Medical and Dental Sciences, Kagoshima University, Kagoshima, Japan

ARTICLE INFO

Article history:
Received 17 December 2012
Accepted 28 January 2013
Available online 5 February 2013

Keywords:
Marmoset CYP2B6
cDNA cloning
Bupropion
Efavirenz
Docking simulation

ABSTRACT

The common marmoset is a promising species for evaluating the safety of drug candidates. To further understand the capacity for drug metabolism in marmosets, a cDNA encoding a CYP2B enzyme was cloned from the total RNA fraction of marmoset liver by 3′- and 5′-RACE methods. Nucleotide and deduced amino acid sequences showed 90.8 and 86.2% identity, respectively, with human CYP2B6. The marmoset CYP2B6 (marCYP2B6) protein was expressed in insect cells, and its enzymatic properties were compared with those of human (humCYP2B6) and cynomolgus monkey (cynCYP2B6) orthologs in liver and insect cell microsomes. Enzymatic functions were examined for the oxidation of 7-ethoxy-4-(trifluoromethyl)coumarin (7-ETC), bupropion (BUP) and efavirenz (EFV). The kinetic profiles for the oxidation of the three substrates by liver microsomal fractions were similar between humans and cynomolgus monkeys (biphasic for 7-ETC and monophasic for BUP and EFV), but that of marmosets was unique (monophasic for 7-ETC and biphasic for BUP and EFV). Recombinant enzymes, humCYP2B6 and cynCYP2B6, also yielded similar kinetic profiles for the oxidation of the three substrates, whereas marCYP2B6 showed activity only for 7-ETC hydroxylation. *In silico* docking simulations suggested that two amino acid residues, Val-114 and Leu-367, affect the activity of marCYP2B6. In fact, a marCYP2B6 mutant with substitutions V114I and L367V exhibited BUP hydroxylase activity that was 4-fold higher than that of humCYP2B6, while its EFV 8-hydroxylase activity was only 10% that of the human enzyme. These results indicate that the amino acids at positions 114 and 367 affect the enzymatic capacity of marmoset CYP2B6.

1. Introduction

In the drug development process, it is important to understand the toxicities of a candidate as well as its pharmacological effects in the early stages. Though the availability of various kinds of recombinant human drug-metabolizing enzymes makes it possible to predict a fairly accurate metabolic profile for a drug candidate, a total safety evaluation of the candidate should be performed *in vivo* using experimental animals. The animal data obtained can be extrapolated into humans. Therefore, the choice of experimental animals is a key point to obtaining a reliable estimation of the possible toxicity of drug candidates. From this view point, monkeys are thought to be appropriate animal models of humans.

The common marmoset is a promising experimental animal species for safety evaluation and metabolism of drug candidates because of its small body size, and easy of handling and breeding, clear advantages over cynomolgus monkeys and rhesus monkeys which are too big to handle and have poor fertility. However, cumulative data on drug-metabolizing enzymes are rather scarce for common marmosets.

Cytochrome P450 (CYP) is a key enzyme in the oxidation of a number of exogenous and endogenous compounds including drugs [1,2]. Major human drug-metabolizing type CYP enzymes are CYP1A2, CYP2A6, CYP2B6, CYP2C8, CYP2C9, CYP2C19, CYP2D6, CYP2E1 and CYP3A4, accounting for more than 90% of oxidative

Abbreviations: CYP, cytochrome P450; marCYP2B6, marmoset CYP2B6; humCYP2B6, human CYP2B6; cynCYP2B6, cynomolgus monkey CYP2B6; 7-ETC, 7-ethoxy-4-(trifluoromethyl)coumarin; BUP, bupropion; EFV, efavirenz; RACE, rapid amplification of cDNA ends; ss-cDNA, single strand cDNA; fp_2, NADPH-cytochrome P450 reductase.

* Corresponding author at: 1-1-1 Tsushima-naka, Kita-ku, Okayama 700-8530, Japan. Tel.: +81 86 251 7942; fax: +81 86 251 7942.
E-mail address: shizuo@pharm.okayama-u.ac.jp (S. Narimatsu).

0006-2952/$ – see front matter © 2013 Elsevier Inc. All rights reserved.
http://dx.doi.org/10.1016/j.bcp.2013.01.024

drug metabolism [3,4]. In cynomolgus monkeys, many kinds of drug-metabolizing type CYP enzymes are expressed in various organs or tissues, and a total of 23 CYP cDNAs in the CYP1 to 4 families have been registered in GenBank [5]. In marmosets, cDNA nucleotide sequences and deduced amino acid sequences for eight drug-metabolizing type CYP enzymes [CYP1A2 (accession number D86475), CYP2C8 (AB242600), CYP2D19 (D29822), CYP2D30 (AY082602), CYP2E1 (D86477), CYP3A4 (D31921), CYP3A5 (EF589801) and CYP3A90 (EF589800)] have been registered in GenBank to date. Previous studies have characterized the enzymatic functions of marmoset CYP1A2 [6,7], CYP2C8 [8], CYP2D19 [9–11] and CYP2D30 [10] expressed in various heterologus expression systems, but no reliable experimental data have been published on the enzymatic functions of recombinant marmoset CYP2E1 or CYP3A enzymes so far.

In the present study, we focused on CYP2B enzymes in marmoset livers, because only very little information has been reported on the marmoset CYP2B family. Among the nine major hepatic human drug-metabolizing type CYP enzymes, CYP2B6 accounts for 2–6% of total hepatic CYP content and 8–10% of drug oxidation catalyzed by CYP enzymes [12]. Human CYP2B6 (humCYP2B6) catalyzes the oxidation of clinically prescribed drugs such as bupuropion (BUP) [13], an antidepressant, efavirenz (EFV) [14], an anti-HIV drug, and cyclophosphamide [15], an anticancer drug. Furthermore, insecticides such as chlorpyrifos [16] and endosulfan-α [17] are also oxidized by CYP2B6. Therefore, humCYP2B6 is a unique enzyme that contributes to the oxidation not only of clinically important drugs but also of agricultural chemicals [12].

In contrast, the enzymatic properties of cynologus monkey CYP2B6 (cynCYP2B6) have not been fully elucidated, though its nucleotide and deduced amino aid sequences have been revealed (GenBank accession No. DQ074793). Moreover, there is little information about a marmoset ortholog of humCYP2B6 except for the existence of proteins in marmoset liver microsomal fractions revealed by immunoblot analyses [9,18]. The characterization of marmoset CYP enzymes as orthologs of human enzymes is a great help to further understanding the drug-metabolizing capacity of marmosets, which promotes their usefulness as an experimental animal in the research field of drug metabolism and toxicity especially in drug development. If the enzymatic functions of a marmoset enzyme are different from those of the human ortholog, the search for the molecular mechanism(s) causing the difference may bring about the elucidation of enzyme reaction mechanism(s). We thus conducted the present study to clone a cDNA encoding a novel marmoset ortholog of humCYP2B6, express its protein in insect cells and characterize its enzymatic properties, which were compared with those of humCYP2B6 and cynCYP2B6.

2. Materials and methods

2.1. Materials

7-Ethoxy-4-(trifluoromethyl)coumarin (7-ETC) was obtained from Anaspec Inc. (Fremont, CA); 7-hydroxy-4-(trifluoromethyl)-coumarin was from Sigma–Aldrich (St. Louis, MO); BUP hydrochloride and hydroxybupuropion were from Toronto Research Chemicals (North York, ON, Canada); and EFV and 8-hydroxyefavirenz were from Santa Cruz Biotechnology (Santa Cruz, CA). Pooled liver microsomal fractions from humans, cynomolgus monkeys and common marmosets were purchased from BD Biosciences (San Jose, CA). The RNeasy Mini kit, QIA shredder, and MiniElute gel extraction kit were obtained from Qiagen (Valencia, CA). RNA PCR kit (AMV) ver. 3.0, Ex Taq DNA Polymerase HS, DNA ligation kit ver. 2.1, 3′-Full RACE Core set and *Hin*dIII were from TaKaRa Bio (Shiga, Japan); KOD-Plus DNA Polymerase from Toyobo (Tokyo, Japan); Bac-to-Bac Baculovirus Expression System, Cellfection II, High Five cells, 5′-RACE system for rapid amplification of cDNA ends, version 2.0 from Invitrogen (Carlsbad, CA): pGEM-T Easy Vector system from Promega (Madison, WI); Quantum Prep Plasmid Miniprep kit from BIO-RAD (Hercules, CA); cytochrome *c* (type V) from Sigma–Aldrich (St. Louis, MO); aprotinin solution and leupeptin hemisulfate monohydrate and β-NADPH from Wako Pure Ind. (Osaka, Japan); and Big Dye Terminator v. 3.1 Cycle Sequencing kit from Applied Biosystems (Foster City, CA). Primers used in PCR were synthesized by Sigma–Aldrich Japan (Tokyo, Japan). Male adult common marmoset livers were supplied by Professor A. Miyata, Kagoshima University (Kagoshima, Japan). The study was approved by the Institutional Animal Care and Use Committee of Kagoshima University. Other reagents used were of the highest quality commercially available.

2.2. Sequencing of marmoset CYP2BX cDNA

Total RNA was extracted from marmoset liver with the RNeasy Mini kit and QIA shredder according to the manufacturer's directions. A portion of the total RNA was reverse-transcribed using the RNA PCR kit (AMV) ver 3.0 to obtain single-strand cDNA. A partial fragment of cDNA (250 ng) encoding the marmoset CYP2B enzyme was amplified by polymerase chain reaction (PCR) from the single-strand cDNA using the forward primer, 5′-CTGCAGATG-GATAGAAGAGGCCTAC-3′ and the reverse primer, 5′-GTATTTGAG-CTTGAGCAGGAAGCCG-3′, designed based on two regions in CYP2B cDNA that are highly homologous in different species, such as humans (accession number, AC023172), cynomolgus monkeys (DQ074793) and rhesus monkeys (MN_001040212) in the GenBank database. PCR by KOD-Plus DNA polymerase consisted of initial denaturation at 94 °C for 120 s followed by 30 cycles of denaturation at 94 °C for 15 s, annealing at 58 °C for 60 s and extension at 68 °C for 50 s. The PCR product was introduced into the pGEM-T Easy vector using TA cloning, and sequenced in both forward and reverse directions.

3′-RACE for marCYP2BX was performed using the 3′-Full Race Core Set according to the manufacturer's instructions. Gene-specific primers (GSP1 and GSP2 for 3′-RACE, Table 1) were designed based on the nucleotide sequence of a partial fragment of marCYP2BX cDNA amplified by PCR using the primers for the previous step. Single-strand cDNA was synthesized from marmoset liver total RNA using the Oligo(dT) 3′ site adaptor primer (SAD, Table 1). Amplification in the first PCR was primed using first-strand cDNA as a template with GSP1 and the 3′ site adaptor primer (Table 1). PCR by Ex Taq DNA Polymerase consisted of initial denaturation at 94 °C for 120 s followed by 30 cycles of denaturation at 94 °C for 15 s, annealing at 56 °C for 50 s and extension at 68 °C for 240 s. The PCR product was used as a template for nested PCR, and the amplification was primed using the GSP2 and 3′ site adaptor primer under the same PCR conditions. The PCR product was introduced into the pGEM-T Easy vector using TA cloning and sequenced in both forward and reverse directions.

5′-RACE for marCYP2BX was performed using the 5′-RACE System according to the manufacturer's directions. Gene-specific primers (GSP1, GSP2 and GSP3 for 5′-RACE, Table 1) were designed based the nucleotide sequence of a partial fragment of marCYP2BX cDNA amplified by PCR using the primers for the previous step. Single-strand cDNA was synthesized from marmoset liver total RNA using GSP1, and the oligo(dC) tail was introduced at the 3′-end. Amplification in the first PCR was primed using oligo(dC) tailed single-strand cDNA with the abridged anchor primer (AAP, Table 1) and GSP2 primer. PCR by Ex Taq DNA Polymerase consisted of initial denaturation at 94 °C for 120 s followed by 30 cycles of denaturation at 94 °C for 35 s, annealing at 55 °C for 60 s

Table 1
Oligonucleotide primers used for cDNA cloning of marmoset CYP2BX and human CYP2B6.

Primer	Sequence	Target
Homo-CYP2BX-FP	5′-CTGCAGATGGATAGAAGAGGCCTAC-3′	Partial fragment
Homo-CYP2BX-RP	5′-GTATTTGAGCATGAGCAGGAAGCCG-3′	
3′-GSP1	5′-CATGGAAAAGGAGAAATCCAACCCAC-3′	3′-RACE
3′-GSP2	5′-CCACACAGTGAATTCCAACCACCAG-3′	
3′-SAD	5′-CTGATCTAGAGGTACCGGATCC-3′	
5′-GSP1	5′-GGTTTTTACGTATTTG-3′	5′-RACE
5′-GSP2	5′-GAGAAGAGCTCGAACAGCTGGCTGAATAAAG-3′	
5′-GSP3	5′-CTCTTTGTGTCTTGGTACTCAAAGCGTTTTCC-3′	
5′-AAP	5′-GGCCACGCGTCGACTAGTACGGGIIGGGIIGGGIIG-3′	
5′-AUAP	5′-GGCCACGCGTCGACTAGTAC-3′	
marCYP2BX-FP	5′-GGATCC*AAAA*ATGGAGCTCACCGTCTTC-3′	Full-length
marCYP2BX-RP	5′-GGATCCTCAGCGGGCAGGAAGC-3′	
humCYP2B6-FP	5′-GGATCC*AAAAAA*ATGGAACTCAGCGTCCTC-3′	Full-length
humCYP2B6-RP	5′-GGATCCGCGGGCAGGATC-3′	

Underlined and italic letters indicate the restriction enzyme (*Bam*H I) site and Kozak sequence, respectively.

and extension at 72 °C for 210 s with the final extension at 72 °C for 360 s. The PCR product was used as a template for nested PCR, and the amplification was primed using the abridged universal amplification primer (AUAP, Table 1) and GSP3 primer. PCR by Ex Taq HS DNA Polymerase consisted of initial denaturation at 94 °C for 90 s followed by 30 cycles of denaturation at 98 °C for 35 s, annealing at 57 °C for 60 s and extension at 72 °C for 210 s. The PCR product was introduced into the pGEM-T Easy vector using TA cloning and sequenced in both forward and reverse directions.

2.3. Cloning of human fp_2, human and cynomolgus monkey CYP2B6 and marCYP2BX cDNAs

The full-length cDNA encoding human fp_2 was amplified by PCR from human fp_2 cDNA cloned into the pGEM-3Z vector [19] as a template using the forward primer 5′-CCCAAGCTTGGGAAAAAAATGGGAGACTCC-3′ and the reverse primer 5′-GGGGTACCCCCTAGCTCCACACGTCC-3′ (underlined letters are the *Hin*dIII sites). The PCR product was directly introduced into the pGEM-T Easy vector using TA cloning and sequenced in both forward and reverse directions to confirm that there were no PCR errors. The DNA fragment corresponding to human fp_2 was inserted into the cloning site for the P_{10} promoter of the pFastBac Dual vector.

humCYP2B6 cDNA was amplified by PCR from humCYP2B6 cDNA cloned into the p-ENTR/D-TOPO vector [20] as a template employing humCYP2B6-1 FP and RP as forward and reverse primers, respectively in Table 1. The same primers were also employed in the amplification of cynCYP2B6 cDNA. Single-strand cDNAs were synthesized from cynomolgus monkey and marmoset liver total RNA using the oligo(dT) adaptor primer. Full-length CYP2B6 cDNAs of the cynomolgus monkey and marmoset were amplified by PCR using Ex Taq DNA Polymerase from the respective liver single-strand cDNAs as a template using forward and reverse primers (Table 1). The PCR products of humCYP2B6, cynCYP2B6 and marCYP2BX cDNAs were directly introduced into the pGEM-T Easy vector using TA cloning and sequenced in both forward and reverse directions to confirm that there were no PCR errors. The cDNA fragments corresponding to humCYP2B6, cynCYP2B6 and marCYP2BX cDNAs were cut from the pGEM-T Easy plasmids with *Bam*H I and subsequently subcloned into a pFastBac Dual vector containing human fp_2 cDNA digested with *Bam*H I. The expression plasmids were sequenced to verify the correct orientation with respect to the promoter (polyhedrin promoter) for the pFastBac Dual vector.

A recombinant baculovirus carrying human, cynomolgus monkey or marmoset CYP2B6 cDNA was prepared employing the Bac-to-Bac Expression System according to the manufacturer's instructions. For protein expression, High Five cells (4×10^8 cells/200 mL) were infected with recombinant baculoviruses at a multiplicity of infection of 2.0, followed by cultivation for 72 h with fortifying 50 mM δ-aminolevulinic acid and 50 mM ferric citrate 24 h after infection. The cells were then harvested, and suspended in 50 mM Tris–HCl buffer (pH 7.4) containing 250 mM sucrose, 0.1 mM EDTA, 0.1 mM DTT, 0.1% aprotinin and 1 μg/mL leupeptin, and stored at −80 °C prior to use. For the preparation of microsomal fractions, the cells were quickly thawed in a water bath at 37 °C, sonicated 40 times with 5-s bursts in ice, and centrifuged at $600 \times g$ for 10 min. The supernatant was successively centrifuged at $9000 \times g$ for 20 min and then at 105,000 × *g* for 60 min at 4 °C. The resultant pellet was resuspended in 50 mM potassium phosphate buffer (pH 7.4) containing 1 mM DTT, 1 mM EDTA and 20% glycerol, and stored at −80 °C until used. Protein concentrations were determined by the method of Lowry et al. [21] using bovine serum albumin as a standard.

2.4. Assay for recombinant CYP2B6 and fp_2 contents

Microsomal fractions from insect cells expressing each primate CYP2B6 was diluted to 2.5–3.0 mg protein/mL with 100 mM potassium phosphate buffer (pH 7.4) containing 20% (v/v) glycerol, and functional CYP content was measured spectrophotometrically by the method of Omura and Sato [22] using 91 mM^{-1} cm^{-1} as the absorption coefficient. Using the same microsomal fractions, the reduction of cytochrome c by fp_2 in the presence of NADPH was measured according to the method of Thor et al. [23] using 21 mM^{-1} cm^{-1} as the absorption coefficient.

Pooled microsomal fractions from human, cynomolgus monkey and marmoset livers (each 60 μg protein) and insect cell microsomal fractions (each 3 μg) were subjected to 10% sodium dodecyl sulfate-polyacrylamide gel electrophoresis (SDS-PAGE) [24]. Proteins on the gel were electroblotted to a polyvinylidene difluoride membrane (Millipore, Billerica, MA), and analyzed by Western blotting according to a published method [25] using sheep anti-human CYP2B6 peptide (Ile265-Lys276) antibody (BIOMOL, Hamburg, Germany) as a primary antibody and horseradish peroxidase-conjugated rabbit anti-sheep IgG (H + L) as a secondary antibody. Proteins were visualized with chemifluorescence using the ELC Plus Western blotting Detection System (GE Healthcare Japan, Tokyo, Japan).

2.5. Enzymatic assay

7-ETC *O*-deethylation activity was determined by the HPLC method of Jinno et al. [20] with a slight modification. The ice-cold reaction mixture (500 μl) contained 10 mM G-6-P, 2 IU of G-6-P dehydrogenase, 5 mM $MgCl_2$, 0.2 mM EDTA, 0.5 mM $NADP^+$, microsomes [HLM (200 μg protein), CLM (60 μg protein, MLM (20 μg protein) and recombinant enzymes (each 200 μg protein)] and 7-ETC (0.1–50 μM) in 50 mM potassium phosphate buffer (pH 7.4). After preincubation at 37 °C for 1 min, the reaction was initiated by adding the NADPH-generating system, followed by incubation at 37 °C for 10 min. The reaction was stopped by adding ice-cold 10% phosphoric acid, and the reaction tube was centrifuged at 12,000 × *g* for 10 min at 4 °C. The supernatant was passed through a PTFE membrane (pore size 0.45 μm, Milipore), and a part of the filtrate was subjected to HPLC under the conditions described below.

BUP hydroxylation activity was measured by the HPLC method of Hesse et al. [13] with a slight modification. The ice-cold reaction mixture (500 μl) contained the same ingredients described for the 7-ETC oxidation assay except the enzyme sources (liver microsomes HLM, CLM and MLM 200 μg protein each; recombinant enzymes 200 μg protein each) and substrate (BUP 5–2000 μM). After preincubation at 37 °C for 1 min, the reaction was initiated by adding the NADPH-generating system, followed by incubation at 37 °C for 20 min. The reaction mixture was treated as described above for the following HPLC analysis.

EFV 8-hydroxylaion activity was determined by the HPLC method of Ward et al. [14] with a slight modification. The ice-cold reaction mixture (200 μl) contained the same ingredients described for the 7-ETC oxidation assay except the enzyme sources [liver microsomes HLM and MLM (500 μg protein each), CLM (200 μg protein); recombinant enzymes, humCYP2B6 and cynCYP2B6 (500 μg protein each), marCYP2B6 (1 mg protein)] and substrate (EFV 0.5–200 μM). After preincubation at 37 °C for 2 min, the reaction was initiated by adding the NADPH-generating system, followed by incubation at 37 °C for 20 min. The reaction mixture was treated as described above for the following HPLC analysis.

2.6. HPLC analysis

HPLC conditions were: a Shimadzu LC-9A liquid chromatograph equipped with a SIL-6B autoinjector, SCL-6B system controller, CTO-10AS column oven and SPD10A UV detector or a Hitachi L2480 fluorescence detector with Smart Chrom data processor (KYA Technologies, Tokyo, Japan). For 7-ETC *O*-deethylation: column, Inertsil ODS-SP (5 μm, 4.6 mm i.d. × 150 mm, GL Sciences, Tokyo, Japan); mobile phase, 20 mM $NaClO_4$ (pH 2.5)/CH_2CN (48:52, by volume); flow rate, 1.0 mL/min; detection, fluorescence excitation/emission wavelengths 342/495 nm; injection volume, 20 μL; column temperature, 40 °C. For BUP hydroxylation: column, Inertsil ODS-SP (5 μm, 4.6 mm i.d. × 150 mm); mobile phase, 50 mM KH_2PO_4 (pH 3.0)/CH_3CN (80:20, by volume); flow rate, 1.0 mL/min; detection, UV 214 nm; injection volume, 20 μL; column temperature, 40 °C. For EFV 8-hydroxylation: column, Inertsil ODS-SP (5 mm, 4.6 mm i.d. × 150 mm); mobile phase, 50 mM KH_2PO_4 (pH 2.4)/CH_3CN (54:46, by volume); flow rate, 1.0 mL/min; detection, UV 214 nm; injection volume, 50 μL; column temperature, 40 °C.

2.7. Data analysis

Kinetic parameters (apparent K_m and V_{max} values) for the oxidation of 7-ETC, BUP and EFV were calculated by Michaelis–Menten and Eadie–Hofstee plots using Prism v. 5.02 (Graph Pad Software, San Diego, CA) and SigmaPlot v.8.02 (Systat Software, San Jose, CA). All values are represented as the mean ± S.D. for three separate experiments. Statistical comparisons were made with Student's *t*-test, and a difference was considered statistically significant when the p value was <0.05.

2.8. Docking simulation

The homology model of marCYP2B6 was constructed by Swiss-Model (http://swissmodel.expasy. org/) using the crystallographic data for human CYP2B6 (3IBD) obtained from the Protein Data Bank (http://www.rcsb.org/pdb/) and the primary amino acid sequence of marCYP2B6 determined in this study. Hydrogen atoms were added for the homology model using the Biopolymer module of the Insight II software package (Molecular Simulations Inc., San Diego, CA). Six peptides of marCYP2B6 (Arg-97 to Asn-116, Met-198 to Ser-209, Phe-234 to Leu-239, Gly-289 to Ser-303, Ile-359 to His-368, and Thr-469 to Ser-478) were extracted as substrate recognition sites (SRSs) [26]. The active-site cavities of human CYP2B6 and marCYP2B6 were made manually above the sixth ligand of heme at a resolution of 1.0 Å using a homemade CG program working on a Windows PC as described elsewhere [8]. The substitution of amino acid residues was performed using Swiss-pdb Viewer 3.7 (GlaxoSmithKline, http://www.genebee.msu.su/spdbv/mainpage.htm). The amino acid residues at the active sites of hum- and marCYP2B6s were drawn using Accelrys ViewerLite 5.0 (Accelrys Inc., San Diego, CA). The making of the three-dimensional structures of the substrates (7-ETC, BUP and EFV) and their energy minimization were carried out with Winmostar V3.806c (http://winmostar.com/). Docking simulation of the substrates within the active-site cavities of CYP2B6s were performed using Autodock 4.0 and Autodock Tools (ADT) v1.5.4 (Scripps Research Institute, http://autodock.scripps.edu/) and Insight II.

3. Results

3.1. cDNA cloning

cDNA encoding humCYP2B6 contained in the pENTR/D-TOPO plasmid was subcloned into the pGEM-T Easy vector, while cDNA encoding cynCYP2B6 was cloned into the pGEM-T Easy vector from total RNA of the liver of a male adult cynomolgus monkey. The nucleotide sequences were confirmed *via* sequencing to be the same as those of humCYP2B6 (GenBank accession number AC023172.1) and cynCYP2B6 (DQ074793). Because there was no information on a marmoset ortholog of human CYP2B6, we employed 3′- and 5′-RACE methods using primer sets for highly conserved nucleotide sequences of human and cynomolgus monkey CYP2B6 cDNAs in combination with nested PCR. As a result, a single strand cDNA encoding the marmoset CYP2B enzyme (tentatively named CYP2BX) was obtained. The cDNA nucleotide sequence and its deduced amino acid sequence are shown in Fig. 1. Fig. 2 shows a comparison of the amino acid sequences of CYP2BX, cynCYP2B6 and humCYP2B6. Table 2 summarizes the homology between the nucleotide and amino acid sequences of the three proteins. marCYP2BX and humCYP2B6 exhibited 90.8 and 86.2% identity in nucleotide and amino acid sequences, respectively. These sequences were registered with the Cytochrome P450 Nomenclature Committee *via* Dr. David Nelson of The University of Tennessee Health Science Center and DNA Data Base of Japan (DDBJ). The Committee named the protein as marmoset CYP2B6, and DDBJ gave the accession number AB574423.

3.2. Expression of CYP2B proteins in insect cells

The cDNAs encoding human, cynomolgus monkey and marmoset CYP2B6s were inserted into the expression vector pFastBac

```
1     CAGGGCAGTCAGACCAGGACCATGGAGCTCACCGTCTTCCTCTTCTTTGCACTCCTCACA
                          M  E  L  T  V  F  L  F  F  A  L  L  T     13
61    GGCCTTTTGCTTCTCCTGCTCCGGCGTCACCCTAAGGCCCATGGCCGCCTCCCACCAGGC
      G  L  L  L  L  L  L  R  R  H  P  K  A  H  G  R  L  P  P  G     33
121   CCCCGCCCTCTGCCCCTTTTGGGGAACCTTCTGCAGCTGGAGAGAAGAGGCCTACTCAAA
      P  R  P  L  P  L  L  G  N  L  L  Q  L  E  R  R  G  L  L  K     53
181   TCCTTTCTGAAATTCCGAGAGAAATACGGGGATGTCTTCACGGTACACCTGGGACCGAGG
      S  F  L  K  F  R  E  K  Y  G  D  V  F  T  V  H  L  G  P  R     73
241   CCCGTGGTCATGCTGTGTGGAGTGGATGCCATACGGGAGGCCCTGGTGGATCAGGCTGAG
      P  V  V  M  L  C  G  V  D  A  I  R  E  A  L  V  D  Q  A  E     93
301   GTCTTCTCTGGCCGGGGCAAAATTGCCATCGTTGACCCAGTCTTCCAGGGCTACGGCGTG
      V  F  S  G  R  G  K  I  A  I  V  D  P  V  F  Q  G  Y  G  V    113
361   GTCTTTGCCAATGGGGACCGCTGGAAGGCGCTGCGGCGATTCTCTCTGACCACCATGAGG
      V  F  A  N  G  D  R  W  K  A  L  R  R  F  S  L  T  T  M  R    133
421   GACTTTGGGATGGGAAAGCGGAGTGTGGAGGAGCGGATCAAGGAGGAGGCTCAGTGTCTG
      D  F  G  M  G  K  R  S  V  E  E  R  I  K  E  E  A  Q  C  L    153
481   GTGCAGGAGCTTCGGAAATACAAGGGAGCCCTCGTGGACCCCACCTTCTTCTTCCATTCC
      V  Q  E  L  R  K  Y  K  G  A  L  V  D  P  T  F  F  F  H  S    173
541   ATCACCGCCAACATCATCTGCTCCATCGTCTTTGGAAAACGCTTTGAGTACCAAGACAAA
      I  T  A  N  I  I  C  S  I  V  F  G  K  R  F  E  Y  Q  D  K    193
601   GAGTTCCTGAAGCTGCTGCGCTTGTTCTACCAGTCTTTTTCACTTGTCAGCTCTTTATTC
      E  F  L  K  L  L  R  L  F  Y  Q  S  F  S  L  V  S  S  L  F    213
661   AGCCAGCTGTTCGAGCTCTTCTCTGATTTCCTAAAATACTTTCCTGGGGCGCACAGGCAA
      S  Q  L  F  E  L  F  S  D  F  L  K  Y  F  P  G  A  H  R  Q    233
721   ATACGTAAAAACCTGCAGGAAATCGGTGCTTTCATTGGCCACAGTGTGGAGAAGCACCGT
      I  R  K  N  L  Q  E  I  G  A  F  I  G  H  S  V  E  K  H  R    253
781   GAAGCCCTGGACCCCAGCTCCCCCCAGGACCTCATCGACACCTACCTGCTCCACATGGAA
      E  A  L  D  P  S  S  P  Q  D  L  I  D  T  Y  L  L  H  M  E    273
841   AAGGAGAAATCCAACCCACACAGTGAATTCAACCACCAGAATCTCATCTTCAACACGCTC
      K  E  K  S  N  P  H  S  E  F  N  H  Q  N  L  I  F  N  T  L    293
901   TCGCTCTTCTTTGCCGGCACCGAGACCACCAGTACCACTCTCCGCTACGGCTTCCTGCTC
      S  L  F  F  A  G  T  E  T  T  S  T  T  L  R  Y  G  F  L  L    313
961   ATGCTCAAATACCCTCATGTGGCAGAGAGAGTCTACAAGGAGATTGAACAGGTGATTGGC
      M  L  K  Y  P  H  V  A  E  R  V  Y  K  E  I  E  Q  V  I  G    333
1021  CCACATCGCCCTCCAGCATTAGATGACCGAGCCAAAATGCCATACACAGATGCAGTCATC
      P  H  R  P  P  A  L  D  D  R  A  K  M  P  Y  T  D  A  V  I    353
1081  CATGAGATCCAGAGAATTGCTGACCTTCTCCCCATGGGTTTGCCCCACATTGTCACACAA
      H  E  I  Q  R  I  A  D  L  L  P  M  G  L  P  H  I  V  T  Q    373
1141  CACACGAGCTTCCGAGGGTACACCATCCCCAAGGGCACGGAAGTATTTCCCATCCTGAGC
      H  T  S  F  R  G  Y  T  I  P  K  G  T  E  V  F  P  I  L  S    393
1201  ACTGCTCTCAACGACCCACACTACTTTGAAAAACCAGACACCTTCAATCCTGACCACTTT
      T  A  L  N  D  P  H  Y  F  E  K  P  D  T  F  N  P  D  H  F    413
1261  CTGGATACCAATGGGGCACTGAAGAAGAATGAAGCTTTTATCCCCTTCTCCTTAGGGAAG
      L  D  T  N  G  A  L  K  K  N  E  A  F  I  P  F  S  L  G  K    433
1321  CGCATCTGTCTTGGTGAAGGCATCGCCCGCACCGAATTGTTCCTCTTCTTCACCACCATC
      R  I  C  L  G  E  G  I  A  R  T  E  L  F  L  F  F  T  T  I    453
1381  CTCCAAAACTTCTCCGTGGCCAGCCCCGTGGCTCCTGAAGACATCGACCTGACACCCCAG
      L  Q  N  F  S  V  A  S  P  V  A  P  E  D  I  D  L  T  P  Q    473
1441  GAGAATGGTGTGGGCAAACTACCCCCAGCATACCAGATCCGCTTCCTGCCCCGCTGAAGG
      E  N  G  V  G  K  L  P  P  A  Y  Q  I  R  F  L  P  R  *      491
1501  GGCTAAGAAGAGGGGGTCAAGAGATTCCGGGTCATCCAGTTGTCCCCACCTCTGTAGACA

1561  ATGACAATTCCTCCAAAACTTTTGACTGCCCCCTGCAACTTTCTGTTT    1608
```

Fig. 1. Nucleotide and deduced amino acid sequences of marCYP2B6. The numbers of the deduced amino acid and nucleotide sequences are shown on the right and left sides, respectively.

Dual containing human fp_2 cDNA, and each CYP protein was co-expressed with fp_2 in insect High Five cells. Microsomal fractions were obtained and assayed for CYP proteins and functional CYP contents by Western blotting (Fig. 3) and reduced carbon monoxide-difference spectroscopy, respectively. As shown in Fig. 3, single protein bands cross-reacting with anti-humCYP2B6 antibody were observed in the lanes containing pooled human (HLM), cynomolgus monkey (CLM) and marmoset liver microsomes (MLM) in the Western blotting. Furthermore, protein bands were observed also in the lanes containing microsomal fractions of insect cells expressing each of the three recombinant enzymes. The functional CYP contents were 27.7 ± 2.6, 65.2 ± 23.6 and 50.7 ± 11.3 pmol/mg protein for hum-, cyn- and marCYP2B6-expressing insect cell microsomal fractions, respectively. The amount of fp_2 varied from 10.4 ± 3.5 to 26.7 ± 2.4 pmol/mg protein, and the ratio of CYP to fp_2 contained in microsomal fractions was calculated to be 0.2–1.0.

3.3. 7-ETC O-deethylation by liver microsomes and recombinant enzymes

When 7-ETC (0.1–50 μM) was used as a substrate, all of the three liver microsomal fractions examined exhibited oxidative activity as shown in Michaelis–Menten plots (Fig. 4A). Eadie–Hofstee plots yielded biphasic kinetics for human and cynomolgus monkey liver microsomes, but gave monophasic kinetics for marmoset liver microsomes (Fig. 4B). Table 3 (upper column) summarizes kinetic parameters. Kinetic profiles in this index are similar between humans and cynomolgus monkeys, that is, their apparent K_m values for low- and high-K_m phases were close, while

```
humCYP2B6   1   MELSVLLFLA LLTGLLLLLV QRHPNTHDRL PPGPRPLPLL GNLLQMDRRG LLKSFLRFRE KYGDVFTVHL GPRPVVMLCG  80
cynCYP2B6   1   MELSVLLFLA LLTGLLLLLV QRHPNAHGRL PPGPCPLPLL GNLLQMDRRG LLRSFLRFRE KYGDVFTVYL GPRPVVMLCG  80
marCYP2BX   1   MELTVFLFFA LLTGLLLLLL RRHPKAHGRL PPGPRPLPLL GNLLQLERRG LLKSFLKFRE KYGDVFTVHL GPRPVVMLCG  80
                *** * ** * *********   ***  * ** **** ***** *****  *** ** *** *** ******** * **********

                                    SRS1
humCYP2B6  81  VEAIREALVD KAEAFSGRGK IAMVDPFFRG YGVIFANGNR WKVLRRFSVT TMRDFGMGKR SVEERIQEEA QCLIEELRKS  160
cynCYP2B6  81  VEAIREALVD NAEAFSGRGK IAITDPVFQG YGVVFANGNR WKVLRRFSLT TMRDFGMGKR SVEERIQEEA QCLIEELRKS  160
marCYP2BX  81  VDAIREALVD QAEVFSGRGK IAIVDPVFQG YGVVFANGDR WKALRRFSLT TMRDFGMGKR SVEERIKEEA QCLVQELRKY  160
               * ********  ** ****** **  ** * * *** **** * ** ***** * ********** ****** *** ***  ****

                                                        SRS2                          SRS3
humCYP2B6 161 KGALMDPTFL FQSITANIIC SIVFGKRFHY QDQEFLKMLN LFYQTFSLIS SVFGQLFELF SGFLKYFPGA HRQVYKNLQE  240
cynCYP2B6 161 KGALVDPTFL FHSITANIIC SIVFGKRFHY QDQEFLKILN LFYHTFSLAS SMFGQLFELL SGFLKYFPGA HRQVYKNLQE  240
marCYP2BX 161 KGALVDPTFF FHSITANIIC SIVFGKRFEY QDKEFLKLLR LFYQSFSLVS SLFSQLFELF SDFLKYFPGA HRQIRKNLQE  240
              **** ****  * ******** ******** * ** **** *  ***  *** * * * *****  * ******** ***  *****

                                                                SRS4
humCYP2B6 241 INAYIGHSVE KHRETLDPSA PKDLIDTYLL HMEKEKSNAH SEFSHQNLNL NTLSLFFAGT ETTSTTLRYG FLLMLKYPHV  320
cynCYP2B6 241 INAYIGHSVE KHRETLDPSA PQDLIDSYLL QMEKEKSNPH SEFSHRNLII NTLSLFFAGT ETTSTTLRYG FLLMLKYPHV  320
marCYP2BX 241 IGAFIGHSVE KHREALDPSS PQDLIDTYLL HMEKEKSNPH SEFNHQNLIF NTLSLFFAGT ETTSTTLRYG FLLMLKYPHV  320
              * * ****** **** ****  * **** ***  ******* * *** * **   ********** ********** **********

                                                SRS5
humCYP2B6 321 AERVYREIEQ VIGPHRPPEL HDRAKMPYTE AVIYEIQRFS DLLPMGVPHI VTQHTSFRGY IIPKDTEVFL ILSTALHDPH  400
cynCYP2B6 321 AERIYKEIEQ VIGPHRPPAL DDRAKMPYTE AVIHEIQRFA DLLPMGVPHI VTQQTSFRGY IIPKDTEVFP LLSTALHDPH  400
marCYP2BX 321 AERVYKEIEQ VIGPHRPPAL DDRAKMPYTD AVIHEIQRIA DLLPMGLPHI VTQHTSFRGY TIPKGTEVFP ILSTALNDPH  400
              *** * **** ******** *  ********  *** ****   ****** *** *** ******  *** ****   ***** ***

                                  Heme-binding region                                  SRS6
humCYP2B6 401 YFEKPDAFNP DHFLDANGAL KKTEAFIPFS LGKRICLGEG IARAELFLFF TTILQNFSMA SPVAPEDIDL TPQECGVGKI  480
cynCYP2B6 401 YFEKPDTFNP DHFLDANGAL KKNEAFIPFS LGRRMCLGEG IARNELFLFF TTILQNFSVA SPVALEDIDL TPQECGVGKI  480
marCYP2BX 401 YFEKPDTFNP DHFLDTNGAL KKNEAFIPFS LGKRICLGEG IARTELFLFF TTILQNFSVA SPVAPEDIDL TPQENGVGKL  480
              ****** *** ***** **** ** ******* ** * ***** *** ****** ******** * **** ***** **** ****

humCYP2B6 481 PPTYQIRFLPR 491
cynCYP2B6 481 PPTYQIRFLPR 491
marCYP2BX 481 PPAYQIRFLPR 491
              ** ********
```

Fig. 2. Alignment of three amino acid sequences of CYP2B6s. humCYP2B6 is from humans (GenBank Accession No. AC023172) and cynCYP2B6 from cynomolgus monkeys (No. DQ074793). (*) Amino acid residues conserved among the three CYP2B6s.

the V_{max} and CL_{int} values were significantly higher in cynomolgus monkeys than in humans. The K_m value for marmoset liver microsomes (0.32 μM) was close to that for the low-K_m phase of humans and cynomolgus monkeys (0.12–0.18 μM).

Fig. 5A shows Michaelis–Menten plots for 7-ETC *O*-deethylation where insect cell microsomes instead of liver microsomes were used as enzyme sources. Eadie–Hofstee plots gave monophase kinetics for all of the three recombinant enzymes (Fig. 5B). The apparent K_m values were marCYP2B6 (1.1 μM) < cynCYP2B6 (9.7 μM) ≦ humCYP2B6 (13 μM), whereas V_{max} values were marCYP2B6 (0.5 pmol/min/pmol CYP) ≈ cynCYP2B6 (0.6 pmol/min/pmol CYP) < humCYP2B6 (1.5 pmol/min/pmol CYP), resulting in the highest CL_{int} values for marCYP2B6, followed by humCYP2B6 and cynCYP2B6 (Table 4, upper column).

3.4. BUP hydroxylation by liver microsomes and recombinant enzymes

In BUP hydroxylation at a substrate concentration ranging from 5 to 2000 μM by liver microsomal fractions, different kinetic profiles were observed (Fig. 4C). That is, human and cynomolgus monkey liver microsomes showed monophasic kinetics, whereas marmoset liver microsomes yielded biphasic kinetics in Michaelis–Menten plots (Fig. 4C) and Eadie–Hofstee plots (Fig. 4D). Kinetic parameters are listed in Table 3. The apparent K_m value was smallest for the low-K_m phase of marmoset liver microsomes (2.8 μM), followed by cynomolgus monkey (13 μM) and human (116 μM) liver microsomes. The V_{max} value was highest for cynomolgus monkey (1540 pmol/min/mg protein) followed by human and marmoset liver microsomes.

When the enzyme source was changed from liver microsomes to recombinant enzymes, human and cynomolgus monkey CYP2B6 enzymes exhibited BUP hydroxylase activity, whereas marmoset CYP2B6 did not show any detectable activity under the conditions used (Fig. 5C and D). The Apparent K_m value of humCYP2B6 (116 μM) was 3-fold higher than that (39 μM) of cynomolgus monkey, while the V_{max} value of the human enzyme was about half that of the cynomolgus monkey enzyme (Table 4, middle column).

3.5. EFV 8-hydroxylation by liver microsomes and recombinant enzymes

When EFV (0.5 to 200 μM) was employed as a substrate, human and cynomolgous monkey liver microsomes gave monophasic

Table 2
Identities of nucleotide and deduced amino acid sequences of human and cynomolgus monkey CYP2B6 and marmoset CYP2BX.

	humCYP2B6	cynCYP2B6	marCYP2BX
humCYP2B6		94.4	90.8
cynCYP2B6	91.4		90.9
marCYP2BX	86.2	87.4	

Upper-right values, percent identities of the nucleotide sequences; lower left values, percent identities of the deduced amino acid sequences.

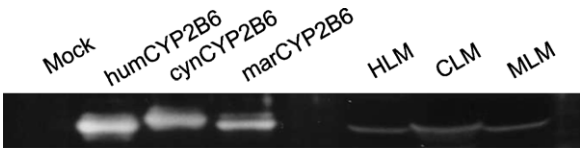

Fig. 3. Western blot analysis of microsomes prepared from human, cynomolgus monkey and marmoset livers, and from insect cells expressing each CYP2B6 protein. Each liver (60 μg) and insect cell (3 μg) microsomal protein sample was applied to a well, and resolved by SDS-PAGE. The proteins were then transblotted to a PVDF membrane and immunochemically probed with polyclonal antibodies raised against human CYP2B6. HLM, CLM and MLM represent human, cynomolgus monkey and marmoset liver microsomes, respectively.

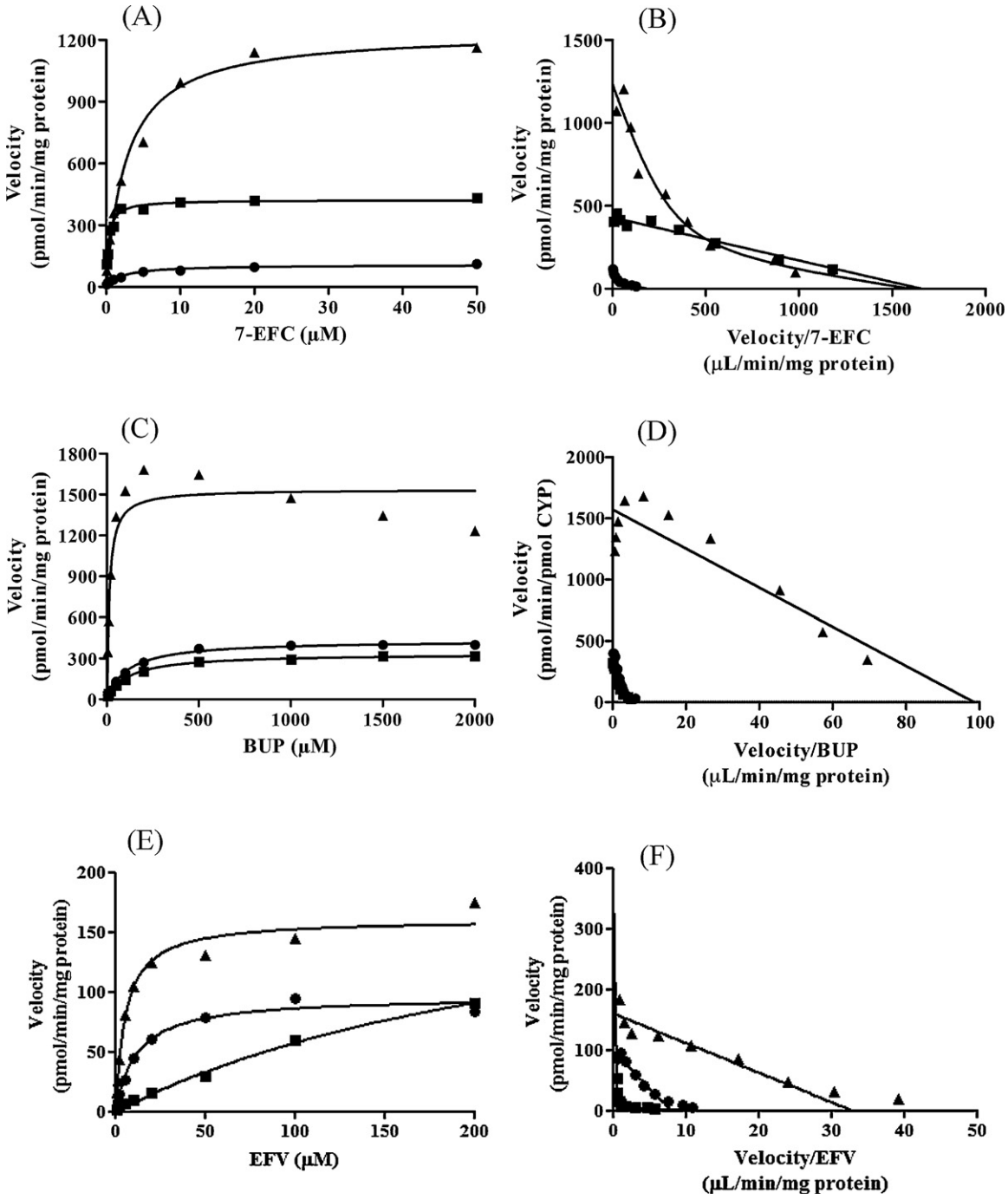

Fig. 4. Typical Michelis–Menten plots (left panels) and Eadie–Hofstee plots (right panels) for the oxidation of 7-ETC (upper panles), BUP (middle panels) and EFV (lower panels) by microsomes from human, cynomolgus monkey and marmoset livers. Closed circles, human; closed triangles, cynomolgus monkey; closed squares, marmoset.

kinetics, whereas EFV oxidation by marmoset liver microsomes was found to be biphasic (Fig. 4E and F). The low-K_m enzyme, which was mainly responsible for EFV 8-hydroxylation in marmoset liver microsomes, had the lowest apparent K_m value (0.5 μM) and the cynomolgus monkey (5.5 μM) and human enzymes (11.5 μM) had 11- and 24-fold, respectively, higher K_m values (Table 3, the lower column). The V_{max} values ranked as follows: marmoset high-K_m enzyme > cynomolgus monkey enzyme > human enzyme > marmoset low-K_m enzyme, resulting in the CL_{int} values: cynomolgus monkey > marmoset ≧ human.

Similar to the case of BUP hydroxylation, marCYP2B6 did not show any detectable EFV 8-hydroxylase activity, while the activity of humCYP2B6 was much higher than that of cynCYP2B6 as shown in Michaelis–Menten (Fig. 5E) and Eadie–Hofstee plots (Fig. 5F). Apparent K_m values were comparable between human and cynomolgus monkey enzymes, whereas the V_{max} values were 11-fold higher for humCYP2B6 than for cynCYP2B6, resulting in a 13-fold higher CL_{int} value for the human enzyme than for monkey enzyme (Table 4, the lower column).

3.6. In silico *search for structural factors affecting enzymatic function of marCYP2B6*

The three-dimensional structure of marCYP2B6 was automatically constructed *via* the web site of Swiss-model (http://swissmodel.expasy.org/) employing the crystal structure of

Table 3
Kinetic parameters for 7-ETC *O*-deethylation, BUP hydroxylation and EFV 8-hydroxylation by human, cynomolgus monkey and marmoset liver microsomes.

		K_m (μM)	V_{max}[a]	CL_{int}[b]
(1) 7-ETC *O*-deethylation				
HLM	Low-K_m phase	0.115 ± 0.072	24.8 ± 8.2	0.215 ± 0.14
	High-K_m phase	5.92 ± 1.30	94.8 ± 5.8	0.016 ± 0.003
CLM	Low K_m phase[c]	0.178 ± 0.035	245 ± 3.5**	1.38 ± 0.13**
	High-K_m phase[d]	5.80 ± 0.99	982 ± 5.7**	0.169 ± 0.003**
MLM		0.323 ± 0.063	424 ± 14	1.36 ± 0.24**
(2) BUP hydroxylation				
HLM		116 ± 13	434 ± 16	3.80 ± 0.56
CML		13.2 ± 2.8**	1540 ± 40**	121 ± 21**
MLM	Low-K_m phase	2.79 ± 0.29	26.6 ± 8.6	9.50 ± 3.00
	High-K_m phase	160 ± 27	318 ± 15	0.503 ± 0.060
(3) EFV 8-hydroxylation				
HLM		11.5 ± 0.07	96.0 ± 2.1	8.36 ± 0.31
CML		5.48 ± 0.76**	160 ± 8.4**	29.9 ± 5.0**
MLM	Low-K_m phase	0.485 ± 0.089	4.21 ± 0.93	9.17 ± 3.4
	High-K_m phase	621 ± 164	355 ± 67	0.588 ± 0.062

HLM, human liver microsomes; CLM, cynomolgus monkey liver microsomes; MLM, marmoset liver microsomes.
[a] pmol/min/mg protein.
[b] nL/min/mg protein. Each value represents the mean ± S.D. for three separate experiments.
[c] Compared with HLM-low-K_m phase.
[d] Compared with HLM-high-K_m phase.
** Significantly different from the human values ($p < 0.01$).

humCYP2B6 (3IBD) as a template. Within substrate recognition sites 1–6, we carefully checked amino acid residues, having side-chains oriented to the active-site cavity, that are different between marmoset and human CYP2B6 proteins. As a result, there is a possibility that two amino acid residues at positions 114 (valine for marmoset and isoleucine for human) and 367 (leucine for marmoset and valine for human) near the heme moiety may affect the shape of the active-site cavity (Fig. 6). We then prepared marCYP2B6 mutants having human-type amino acid residue(s) at positions 114 and/or 367 *in silico* by using Swiss PDB Viewer, and performed a docking simulation study of BUP or EFV within the active-site cavities of the marCYP2B6 wild-type and mutants, and compared the results with those for the human CYP2B6 wild-type protein.

Fig. 7 shows the simulated orientations of 7-ETC, *S*-BUP and *S*-EFV above the heme moiety in the active-site cavity of the humCYP2B6 wild-type (A, C and F), the marCYP2B6 wild-type (B, D and G) and a mutant having double amino acid substitutions (V114I/L367V-marCYP2B6) (E and H). The distances between the heme iron and the oxidation site of each substrate are also shown. The distance between the oxidation site of 7-ETC and the heme iron was 3.5 Å in the active-site cavity of wild-type humCYP2B6 (Fig. 7A), while it was 2.6 Å in the active-site cavity of wild-type marCYP2B6 (Fig. 7B). It is reasonable to assume that the oxidation by CYP that occurs between the heme iron and the oxidation site of the substrate is within 4–5 Å. From this assumption, 7-ETC can be oxidized by both human and marmoset CYP2B6s, and the distance between the heme iron and the oxidation site was shorter in marCYP2B6 than in humCYP2B6, which is well consistent with the experimental results revealing the higher 7-ETC *O*-deethylase capacity for the marmoset enzyme than human enzyme (Table 4).

The oxidation profiles for BUP and EFV are different. That is, the distances between the oxidation site of both substrates and the heme iron in the active-site cavity are larger for the marmoset enzyme than human enzyme. Notably, the distance between the 8-position of *S*-EFV and the heme iron is 9.2 Å for the marCYP2B6 wild-type and 3.8 Å for the human enzyme. Interestingly, the distances between the oxidation sites of *S*-BUP and *S*-EFV have become much shorter in the active-site cavity of V114L/L367V-marCYP2B6, *i.e.*, 4.6 Å → 2.7 Å for *S*-BUP and 9.2 Å → 4.0 Å for *S*-EFV. On the basis of the results obtained from the *in silico* simulation, we then prepared cDNAs encoding marCYP2B6 mutants in which Val-114 and/or Leu-367 were substituted with human type Ile-114 and/or Val-367 by site-directed mutagenesis, and expressed their proteins in the insect cell system.

3.7. The oxidation of BUP and EFV by insect cell microsomal fractions expressing marCYP2B6 mutants

Fig. 8 shows Michaelis–Menten plots for BUP hydroxylation (a left panel) and EFV 8-hydroxylation (a right panel) by marCYP2B6 mutants. Eadie–Hofstee plots for both oxidation reactions gave monophasic profiles (Figures not shown). Of particular interest, all of the single and double amino acid-substituted marCYP2B6 mutants had BUP hydroxylase activity, which was undetectable for the wild-type enzyme. In EFV 8-hydroxylation, however, the single amino acid substituted mutant, V114I-marCYP2B6 did not show detectable activity under the conditions used. Table 5 lists the kinetic parameters calculated. For BUP hydroxylation, apparent K_m values of marCYP2B6 mutants ranged from 68 to 99 μM, which were similar to that of humCYP2B6 (116 μM). Based on V_{max} values of the mutants ranked V114I/L367V > L367V > V114I, in which the value for the L367V-mutant was comparable to that for the human enzyme. As a result, the CL_{int} values of the L367V- and V114I/L367V-mutants were the same as and 3.5-fold higher than, respectively, that of humCYP2D6, while V114I-mutant was much less active than the human enzyme. For EFV 8-hydroxylation, the V114I-mutant did not exert any detectable activity under the conditions employed, while the L367V- and V114I/L367V-mutants were much less active than the human enzyme (Table 5).

4. Discussion

The present study focused on the properties of marmoset and cynomolgus monkey CYP2B6s. As a first step we conducted to clone a cDNA encoding a marmoset ortholog of human CYP2B6 employing 3′- and 5′-RACE methods, succeeding in the cDNA cloning and the protein expression in the insect cells. When we consulted with Dr. Nelson of the Cytochrome P450 Nomenclature Committee on the naming of a novel marmoset CYP2B enzyme, he recommended us to use the name of "CYP2B6". In the home page of Dr. Nelson (http://drnelson.uthsc.edu/biblioA.html#2B), the same nomenclature, "CYP2B6", has been given to seven mammalian CYPs; human, chimpanzee, rhesus monkey, cynomolgus monkey, marmoset (this study), cow and cat. This may be a little confusing when the genes and enzymatic functions of several CYP2B6s are discussed, so we used the terms of humCYP2B6, cynCYP2B6 and marCYP2B6 to distinguish them in the present study. However, it would be convenient for us that each CYP has its own nomenclature to avoid confusion.

As a second step, we kinetically analyzed the oxidation of three substrates, 7-ETC, BUP and EFV, by monkey liver microsomal fractions, and compared the results with those of human liver microsomes. 7-ETC *O*-deethylation was analyzed to be biphasic for human and cynomolgus monkey liver microsomal fractions. Code et al. [27] reported that 7-ETC *O*-deethylation in the human liver was mediated by multiple CYP enzymes including CYP1A2 ($K_m < 0.1$ μM) and CYP2B6 (2.9 μM) as major enzymes, being consonant with the present results. Considering that the K_m values in biphasic kinetics were similar between human and cynomolgus monkey liver microsomal fractions (Table 3), 7-ETC *O*-deethylation in cynomolgus liver microsomes might be mediated by CYP1A2 as a low-K_m enzyme and CYP2B6 as a high-K_m enzyme, respectively. In contrast, marCYP2B6 could be mainly responsible for marmoset liver microsomal 7-ETC *O*-deethylation.

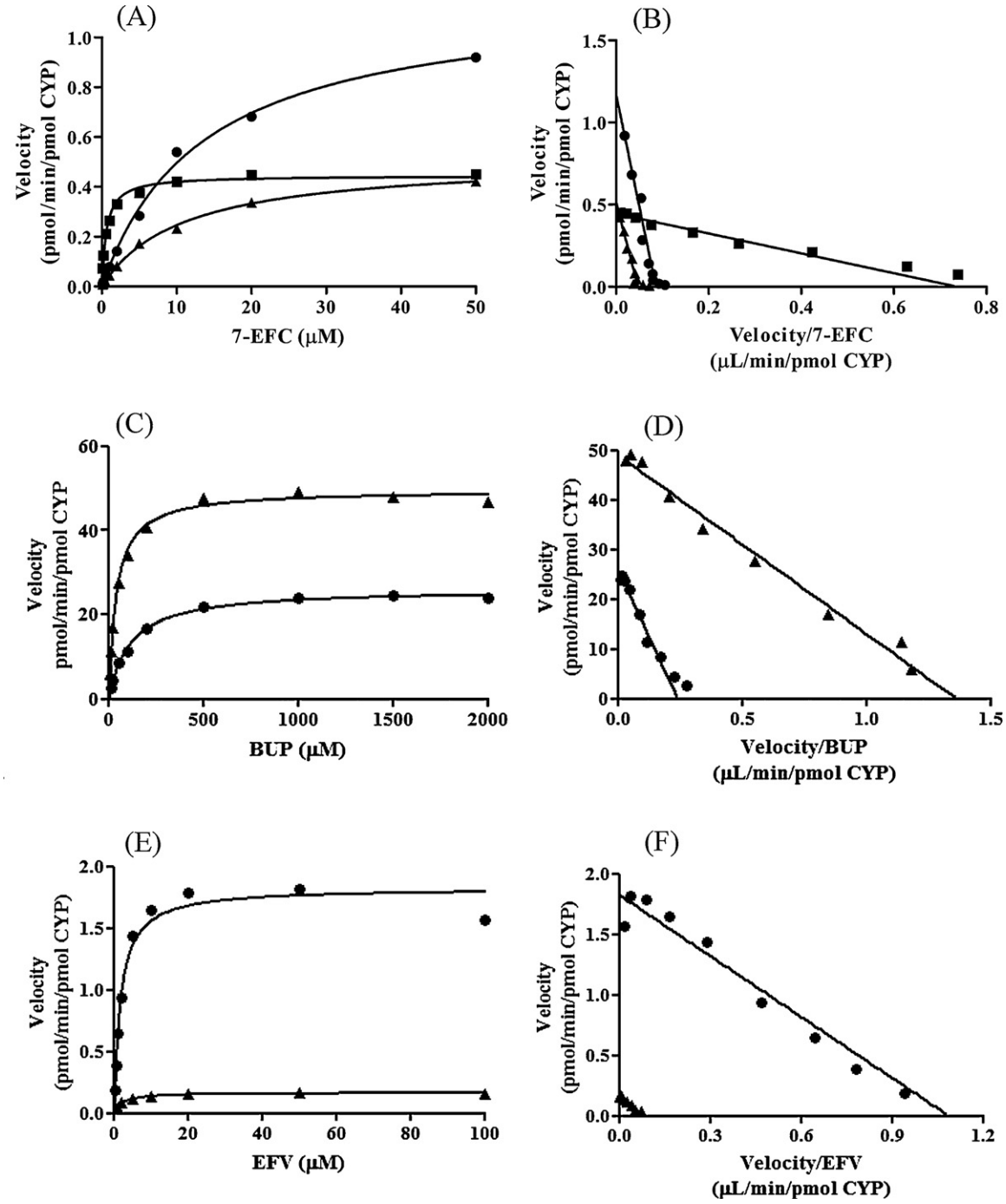

Fig. 5. Typical Michaelis–Menten plots (left panels) and Eadie–Hofstee plots (right panels) for the oxidation of 7-ETC (upper panels), BUP (middle panels) and EFV (lower panels) by microsomes from insect cells expressing humCYP2B6, cynCYP2B6 or marCYP2B6. Closed circles, human; closed triangles, cynomolgus monkey; closed squares, marmoset.

BUP hydroxylation [13,28] and EFV 8-hydroxylation [14,29] have been demonstrated to be catalyzed mainly by CYP2B6 in human liver microsomes. Consonant with the previous findings, both BUP hydroxylation and EFV 8-hydroxylation gave monophasic profiles in human liver microsomes in the present kinetic study. The K_m values for BUP hydroxylation were in good agreement between the human liver microsomes and humCYP2B6, but the values for EFV 8-hydroxylation were considerably different between the human liver microsomes and recombinant enzyme. It is unclear at present what causes the difference.

Cynomolgus monkey liver microsomes also showed monophasic profiles for the oxidation of these substrates. Employing LC/MS analysis, Mutlib et al. [30] observed a similarity in the metabolic profiles of EFV between humans and cynomolgus monkeys. Uno et al. [31] cloned a cDNA encoding cynomolgus monkey CYP2B6 and expressed its proteins in *Escherichia coli*. They found some oxidation activities for testosterone 16α-hydroxylation and BUP hydroxylation by the recombinant enzyme, but did not perform kinetic analysis [31]. Therefore, the present study is the first report describing the kinetic property of cynomolgus monkey CYP2B6. Judging from the K_m values, cynCYP2B6 is

Table 4
Kinetic parameters for 7-ETC *O*-deethylation, BUP hydroxylation and EFV 8-hydroxylation by human, cynomolgus monkey and marmoset CYP2B6s.

	K_m (μM)	V_{max}[a]	CL_{int}[b]
(1) 7-ETC O-deethylation			
humCYP2B6	12.7 ± 3.5	1.51 ± 0.13	126 ± 30
cynCYP2B6	9.65 ± 1.73	0.55 ± 0.03**	52 ± 9**
marCYP2B6	1.05 ± 0.31**##	0.51 ± 0.07**	526 ± 151**##
(2) BUP hydroxylation			
humCYP2B6	116 ± 39	26.5 ± 2.5	251 ± 91
cynCYP2B6	38.9 ± 1.8*	49.5 ± 5.8**	1270 ± 91**
marCYP2B6	N.D.	N.D.	N.D.
(3) EFV 8-hydroxylation			
humCYP2B6	1.66 ± 0.20	1.83 ± 0.34	1092 ± 115
cynCYP2B6	2.04 ± 0.53	0.167 ± 0.021**	85 ± 14**
marCYP2B6	N.D.	N.D.	N.D.

N.D., not detectable. Significantly different from humCYP2B6 ($^{*}p < 0.05$ and $^{**}p < 0.01$). Significantly different from cynCYP2B6 ($^{\#\#}p < 0.01$).
[a] pmol/min/pmol CYP.
[b] nL/min/pmol CYP. Each value represents the mean ± S.D. for three separate experiments.

Table 5
Kinetic parameters for BUP hydroxylation and EFV 8-hydroxylation by marCYP2B6 and three mutants.

	K_m (μM)	V_{max}[a]	CL_{int}[b]
(1) BUP hydroxylation			
humCYP2B6	116 ± 39	26.5 ± 2.5	251 ± 91
marCYP2B6	N.D.	<0.176	N.D.
V114I	98.9 ± 24.9	3.17 ± 0.13*	34.0 ± 7.9
L367V	87.2 ± 4.6	21.8 ± 4.2	250 ± 44
V114I/L367V	67.8 ± 15.0	58.5 ± 12.0**††##	882 ± 191**††##
(2) EFV 8-hydroxylation			
humCYP2B6	1.66 ± 0.20	1.83 ± 0.34	1092 ±115
marCYP2B6	N.D.	<0.05	N.D.
V114I	N.D.	<0.05	N.D.
L367V	4.56 ± 0.84**	0.143 ± 0.002**	32.9 ± 8.9**
V114I/L367V	1.93 ± 0.24##	0.218 ± 0.052**	117 ± 37**

N.D., not detectable. Significantly different from humCYP2B6 ($^{*}p < 0.05$, $^{**}p < 0.01$), from V114I ($^{\dagger\dagger}p < 0.01$), or from L367 V ($^{\#\#}p < 0.01$).
[a] pmol/min/pmol CYP.
[b] nL/min/pmol CYP. Each value represents the mean ± S.D. for three separate experiments.

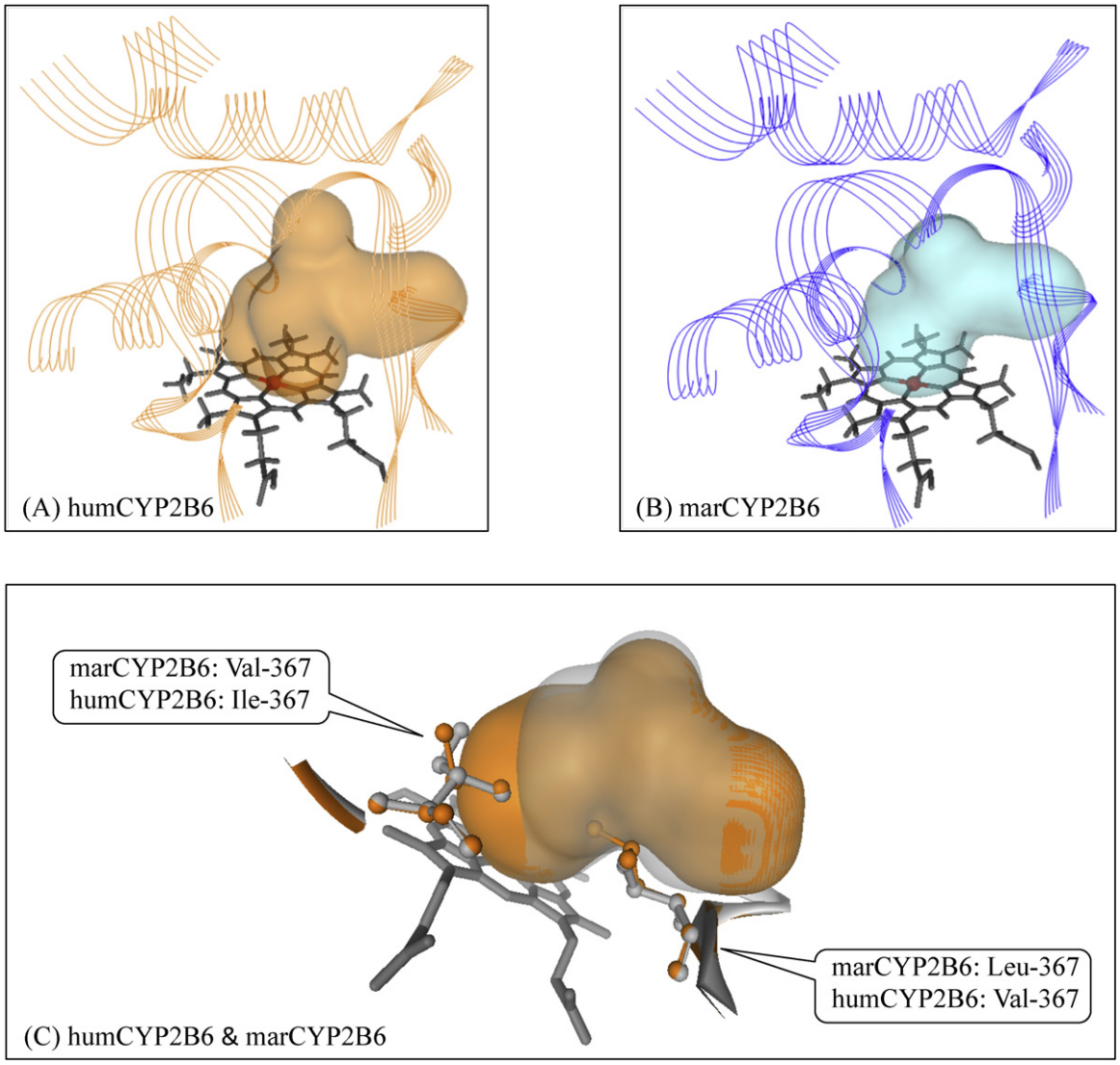

Fig. 6. Comparison of the active-site cavity of humCYP2B6 (A) and marCYP2B6 (B) and speculated amino acid residues which may affect the substrate specificity of the two enzymes by changing the shape of the active-site cavity (C).

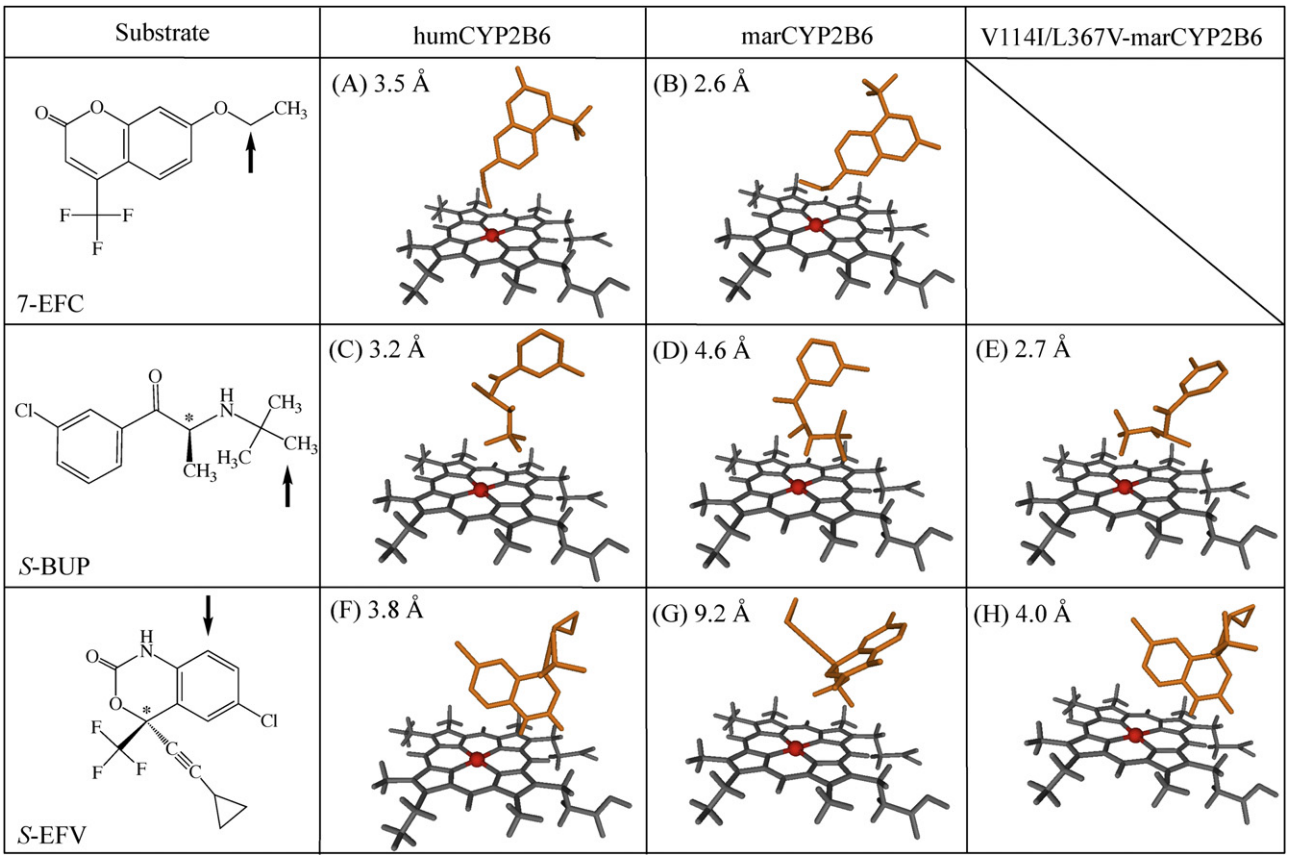

Fig. 7. Orientations of the three substrates within the active-site cavities of humCYP2B6, marCYP2B6 and the V114I/L367V-marCYP2B6 mutant. The optimized orientation for each substrate was obtained by docking simulations using ADT with default genetic algorithm parameters except for individual GA runs, 100. Arrows in left panels, oxidation sites. The value (Å) in each panel showing the orienation of each substrate indicates the distance between the oxidation site of the substrate and the heme iron.

thought to be mainly responsible for the oxidation of BUP and EFV in cynomolgus mokey liver microsomes.

Marmoset liver microsomes, on the other hand, clearly exhibited an oxidative capacity for BUP and EFV, though marCYP2B6 did not show any oxidative activity toward these substrates under the experimental conditions used. These results indicate that some CYP enzyme(s) other than CYP2B6 are responsible for marmoset liver microsomal BUP and EFV oxidation, which are catalyzed mainly by CYP2B6s in human and cynomolgus monkey liver microsomes. On the basis of the CL_{int} values, the oxidation capacity of liver microsomal fractions ranked as follows: cynomolgus monkey ≈ marmoset > humans for 7-ETC, cynomolgus monkey ≫ marmoset > humans for BUP, and cynomolgus monkey > marmoset ≈ humans for EFV (Table 3).

The question arises, "why does not the marmoset enzyme catalyze the oxidation of BUP or EFV?" In search of the molecular mechanism(s) preventing marCYP2B6 from catalyzing BUP or EFV oxidation, we prepared conformations of marCYP2B6 *in silico via* Swiss Model employing the crystal structure of hum CYP2B6 as a template. We carefully compared the shapes of active-site cavities and amino acid residues whose side-chains extrude into the active-site cavities between marCYP2B6 and humCYP2B6, and chose two amino acids, Val-114 and Leu-367, as possible residues that affect the shape of the active-site cavity of the marmoset enzyme, maybe resulting in the change to its catalytic properties.

In the docking simulation employing Autodock 4.0, we used three substrates, 7-ETC, *S*-BUP and *S*-EFV, while we used BUP and EFV racemates as substrates in the *in vitro* enzyme assay. The reason why we employed *S*-BUP and *S*-EFV in the *in silico* study is

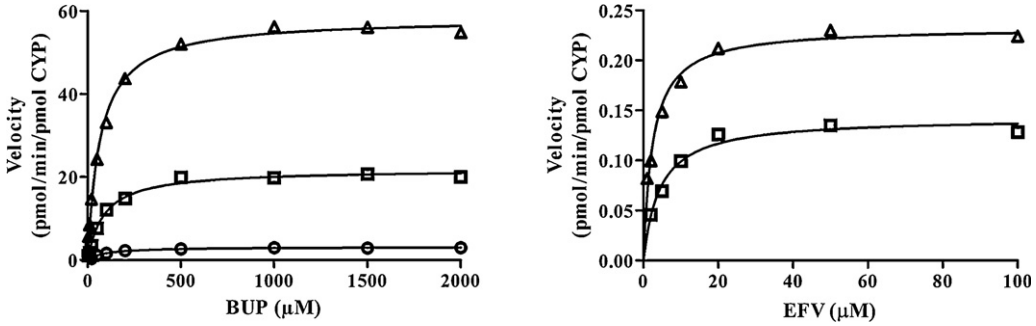

Fig. 8. Typical Michaelis–Menten plots for the oxidation of BUP (left panels) and EFV (right panels) by microsomes from insect cells expressing marCYP2B6 and its three mutants having single and double amino acid substitutions. Open circles, V114I-mutant; open squares, L367V-mutant; open triangles, V114I/L367V-mutant.

that a BUP racemate is used clinically and the hydroxylation of *S*-BUP was 1.5- and 3-fold higher than that of *R*-BUP by human liver microsomes and humCYP2B6, respectively [32] and that *S*-EFV but not *R*-EFV is clinically used as an anti-HIV drug [33].

As shown in Fig. 7, the oxidation sites of BUP and EFV are rather far from the heme iron (4.6 Å and 9.2 Å for BUP and EFV, respectively) in the active-site cavity of the marCYP2B6 wild-type, whereas the distances became closer (2.7 Å and 4.0 Å for BUP and EFV, respectively) in the active-site cavity of the V114I/L367V-mutant. The distance between the oxidation site of BUP and the heme iron (2.7 Å) of the mutant is shorter than that in the humCYP2B6 (3.2 Å), which may result in the greater BUP oxidative capacity of the mutant compared to humCYP2B6 (Table 5). Only the single substitution of Val-114 with isoleucine or of Leu-367 with valine rendered marCYP2B6 the capacity to mediate BUP hydroxylation, though the effect of the latter, in which the CL_{int} value was comparable to that of humCYP2B6, is much greater than the former, in which the CL_{int} value was only 14% that of the human enzyme. Furthermore, the double subsitutions of amino acids at positions 114 and 367 increased the CL_{int} value 3.5-fold compared to those of humCYP2B6 and the L367V-marCYP2B6 mutant. These results may mean that the substitution of Leu-367 with valine is mainly responsible for the increased BUP oxidizing capacity of marCYP2B6, but some concerted effect is produced by the double amino acid substitution, though the effect of the single substitution of Val-114 with isoleucine is rather small.

For EFV 8-hydroxylation, on the other hand, the substitution of amino acids at positions 114 and 367 did not have such a remarkable effect. That is, the V114I-mutant did not exhibit any detectable activity, and the CL_{int} value of the L367V-mutant was only 3% that of humCYP2B6. Even the V114I/L367V-mutant yielded only 10% of the capacity of the human enzyme, though the speculated distance between the oxidation site of EFV and the heme iron is 4.0 Å in the active-site cavity (Fig. 7). It seems that the distance "4 Å" is close to the limit for the oxidation of the substrate to occur in the active-site cavity of marCYP2B6. There is another possibility that some other amino acid residue(s) as well as Val-114 and Leu-367 in the active-site cavity may be involved in the oxidation of EFV by the marmoset enzyme. It should be noted that there has been no reports describing on human CYP2B6 alleles involving amino acid substitutions at positions 114 or 367 [34].

In the present study, various recombinant CYP2B6 proteins were co-expressed with fp_2 in insect cells where the ratios of CYP to fp_2 varied from 0.2 to 1.0 as described in Section 3. Therefore, some activities of the recombinant CYP2B6s could be changed under the conditions where fp_2 is overexpressed to a similar extent in each microsomal preparation. Moreover, we employed Swiss Model and Insight II for making the homology models and Autodock Tools for docking simulation, and found out Val-114 and Leu-367 to be key residues for elevation in BUP and EFV oxidation activities of mar-CYP2B6 in the present study. However, the system that we used has some limitations. For example, though *S*-EFV takes similar special orientations in the active-site cavities between hum-CYP2B6 and V114I/L367V-marCYP2B6 in this model (Fig. 7), the activity of the human enzyme was much higher than that of the marmoset mutant. Additionally, affinity between substrates and enzyme proteins cannot be predicted by this system.

For further elucidation of molecular mechanism(s) involved in the interesting phenomenon found in this study, highly efficient tools are necessary to simulate possible interactions of substrates with amino acid residues in the active-site cavity and to predict the affinity of substrates for CYP enzymes, resulting in more accurate prediction of enzyme activity and selectivity. Cumulated information including the present results increases the usefulness of marmosets in the research of drug metabolism, pharmacokinetics and toxicokinetics for the development of new drug candidates.

In summary, the present study focused on the enzymatic properies of marmoset CYP2B6 and compared them with those of human and cynomolgous monkey orthologs using 7-ETC, BUP and EFV as substrates. The kinetic profiles for the oxidation of the three substrates by liver microsomal fractions were similar between humans and cynomolgus monkeys (biphasic for 7-ETC and monophasic for BUP and EFV), but that of marmosets was unique (monophasic for 7-ETC and biphasic for BUP and EFV). Recombinant enzymes, humCYP2B6 and cynCYP2B6, also yielded similar kinetic profiles for the oxidation of the three substrates, whereas marCYP2B6 showed activity only for 7-TEC hydroxylation. *In silico* docking simulations suggested that two amino acid residues, Val-114 and Leu-367, affect the activity of marCYP2B6. In fact, a marCYP2B6 mutant with the substitutions of V114I and L367V exhibited BUP hydroxylase activity that was 4-fold higher than that of humCYP2B6, while its EFV 8-hydroxylase activity was only 10% that of the human enzyme. These results indicate that the amino acids at positions 114 and 367 affect the enzymatic capacity of marmoset CYP2B6.

Conflict of interest

The authors declare that there are no conflicts of interest.

References

[1] Nebert DW, Russell DW. Clinical importance of cytochrome P450. Lancet 2002;360:1155–62.
[2] Guengerich FP. Cytochrome P450 and chemical toxicology. Chem Res Toxicol 2008;21:70–83.
[3] Evans WE, Relling MV. Pharmacogenomics: tralslating functional genomics into rational therapeutics. Science 1999;286:487–91.
[4] Rendic S. Summary of information on human CYP enzymes: human P450 metabolism data. Drug Metab Rev 2002;34:83–448.
[5] Uno Y, Iwasaki K, Yamazaki H, Nelson DR. Macaque cytochrome P450: nomenclature, transcript, gene, genomic structure, and function. Drug Metab Rev 2011;43:346–61.
[6] Sakuma T, Igarashi T, Hieda M, Ohgiya S, Isogai M, Ninomiya S, et al. Marmoset CYP1A2: primary structure and constitutive expression in livers. Carcinogenesis 1997;18:1985–91.
[7] Narimatsu S, Oda M, Hichiya H, Isobe T, Asaoka K, Hanioka N, et al. Molecular cloning and functional analysis of cytochrome P450 1A2 from Japanese monkey liver: comparison with marmoset cytochrome P450 1A2. Chem Biol Interact 2005;152:1–12.
[8] Narimatsu S, Torigoe F, Tsuneto Y, Saito K, Hanioka N, Masuda K, et al. Cloning of a cDNA encoding a novel marmoset CYP2C enzyme, expression in yeast cells and characterization of its enzymatic functions. Biochem Pharmacol 2006;72:1738–48.
[9] Igarashi T, Sakuma T, Isogai M, Nagata R, Kamataki T. Marmoset liver cytochrome P450s: study for expression and molecular cloning of their cDNAs. Arch Biochem Biophys 1997;339:85–91.
[10] Hichiya H, Kuramoto S, Yamamoto S, Shinoda S, Hanioka N, Narimatsu S, et al. Cloning and functional expression of a novel marmoset cytochrome P450 2D enzyme. CYP2D30: comparison with the known marmoset CYP2D19. Biochem Pharmacol 2004;68:165–75.
[11] Narimatsu S, Nakata T, Shimizudani T, Nagaoka K, Nakura H, Masuda K, et al. Regio- and stereoselective oxidation of propranolol enantiomers by human CYP2D6, cynomolgus monkey CYP2D17 and marmoset CYP2D19. Chemico-Biol Interact 2011;189:146–52.
[12] Wang H, Tompkins LM. CYP2B6: new insights into a historically overlooked cytochrome P450 isozyme. Curr Drug Metab 2008;9:598–610.
[13] Hesse LM, Venkatakrishnan K, Court MH, von Moltke LL, Duan SX, Shader RI, et al. CYP2B6 mediates the in vitro hydroxylation of bupuropion: potentioal drug interactions with other antidepressants. Drug Metab Dispos 2000;28:1176–83.
[14] Ward BA, Gorski JC, Jones DR, Hall SD, Flockhart DA, Desta Z. The cytochrome P450 2B6 (CYP2B6) is the main catalyst of efavirenz primary and secondary metabolism: implication for HIV/AIDS therapy and utility of efavirenz as a substrate marker of CYP2B6 catalytic activity. J Pharmacol Exp Ther 2003;306:287–300.
[15] Roy P, Yu LJ, Crepsi C, Waxman DJ. Development of a substrate-activity based approach to identify the major human liver P-450 catalists of cyclophosphamide and ifosphamide activation based on cDNA-expressed activities and liver microsomal P-450 profiles. Drug Metab Dispos 1999;27:655–66.
[16] Tang J, Cao Y, Rose RL, Brimfield AA, Dai D, Goldstein JA, et al. Metabolism of chlorpyrifos by human cytochrome P450 isoforms and human, mouse, and rat liver microsomes. Drug Metab Dispos 2001;29:1201–4.

[17] Casabar RC, Wallace AD, Hodgson E, Rose RL. Metabolism of endosulfan-alpha by human liver microsomes and its utiliyu as a simultaneous in vitro probe for CYP2B6 and CYP3A4. Drug Metab Dispos 2006;34:1779–85.
[18] Schulz TG, Thiel R, Neubert D, Brassil P, Schulz-Utermoehl T, Boobis AR, et al. Assessment of P450 induction in the marmoset monkey using targeted anti-peptide antibodies. Biochim Biophys Acta 2001;1546:143–55.
[19] Hanioka N, Yamamoto M, Iwabu H, Jinno H, Tanaka-Kagawa T, Naito S, et al. Functional characterization of human and cynomolgus money cytochrome P450 2E1 enzymes. Life Sci 2007;81:1436–45.
[20] Jinno H, Tanaka-Kagawa T, Ohno A, Makino Y, Matsushita E, Hanioka N, et al. Functional characterization of cytochrome P450 2B6 allelic variants. Drug Metab Dispos 2003;31:398–403.
[21] Lowry OH, Rosebrough NJ, Farr AL, Randall RJ. Protein measurement with the Folin phenol reagent. J Biol Chem 1951;193:265–75.
[22] Omura T, Sato R. The carbon monoxide-binding pigment of liver microsomes. I. Evidence for its hemoprotein nature. J Biol Chem 1964;239:2370–8.
[23] Thor H, Smith M, Hartzell P, Bellomo G, Jewell SA, Orrenius S. J Biol Chem 1982 1982;257:12419–24.
[24] Laemmli UK. Cleavage of structural proteins during the assembly of the head of bacteriophage T4. Nature 1970;227:680–5.
[25] Towbin H, Staehelin T, Gordon J. Electrophoretic transfer of proteins from polyacrylamide gels to nitrocellulose sheets: procedure and some applications. Proc Natl Acad Sci USA 1979;76:4350–4.
[26] Gotoh O. Substrate recognition sites in cytochrome P450 family 2 (CYP2) proteins inferred from comparative analyses of amino acid and coding nucleotide sequences. J Biol Chem 1992;267:83–90.
[27] Code EL, Crespi CL, Penman BW, Gonzalez FJ, Chang TH, Waxman DJ. Human cytochrome P4502B6 Interindividual hepatic expression, substrate specificity, and role in procarcinogen activation. Drug Metab Dispos 1997;25:985–93.
[28] Faucette SR, Hawke RL, Shord SS, Lecluyse EL, Lindley CM. Evaluation of the contribution of cytochrome P450 3A4 to human liver microsmal bupropion hydroxylation. Drug Metab Dispos 2001;29:1123–9.
[29] Saussele T, Ward B, Blievernicht J, Li L, Klein K, Flockhart DA, et al. Impact of CYP2B6 polymorphism on hepatic efavirenz metabolism in vitro. Pharmacogenomics 2007;8:547–58.
[30] Mutlib AE, Chen H, Nemeth GA, Markwalder JA, Seitz SP, Gan LS, et al. Drug Metab Dispos 1999;27:1319–33.
[31] Uno Y, Matsuno K, Nakamura C, Utoh M, Yamazaki H. Identification and characterization of CYP2B6 cDNA in cynomolgus macaques (*Macaca fascicularis*). J Vet Med Sci 2009;71:1653–6.
[32] Coles R, Kharasch ED. Stereoselective metabolism of bupuropion by cytochrome P4502B6 (CYP2B6) and human liver microsomes. Pharm Res 2008;25:1405–11.
[33] http://www.healthmash.com/health/efavirenz.html.
[34] http://www.cypalleles.ki.se/cyp2b6.htm.